



## Double-layer-coated stainless steel plates resistant to pitting damage

Masayoshi Kawai<sup>a,\*</sup>, Masatoshi Futakawa<sup>b</sup>, Takashi Naoe<sup>b</sup>, Tsutomu Yamamura<sup>c</sup>, Tadashi Igarashi<sup>d</sup>

<sup>a</sup> KEK, Tsukuba-shi, Ibaraki-ken 305-0801, Japan

<sup>b</sup> Japan Atomic Energy Agency, Tokai-mura, Ibaraki-ken 319-1195, Japan

<sup>c</sup> Tohoku University, Aoba-ku, Sendai-shi 980-8579, Japan

<sup>d</sup> Ion Engineering Research Institute Corp., Hirakata-shi, Osaka-fu 573-0128, Japan

### A B S T R A C T

A serious problem encountered when a liquid-Hg target is used for MW-class pulsed spallation neutron source is pitting damage caused to vessel walls. This pitting damage is due to the impact of cavitation-bubble collapse immediately after intense proton beams are made incident on the target. Pitting damage is thought to be as important as or more important than radiation damage in determining the life time of the target. In the present study, an effectiveness of an SS/Au-double-layer-coated SS plate in reducing pitting damage is investigated. An FEM-analysis reveals that the Au layer absorbs the impact from the surface plate and significantly reduced the stress on the SS substrate. SS/Au/SS specimens are fabricated by using the diffusion bonding method, and the development of pitting damage is investigated by using the MIMTM; the specimens were subjected to 560 W impacts, which produced nearly the same morphology of pitting damage in the MIMTM as that observed in proton-beam tests conducted using MW-class proton beams, for  $10^4$ – $10^6$  cycles. The specimens are then analyzed by EDX for determining the thickness of the diffusion layer and by laser microscopy for detecting micro-cracks and the extent of pitting damage.

© 2009 Elsevier B.V. All rights reserved.

### 1. Introduction

A Hg target system for a pulsed spallation neutron source, JSNS (Japanese Spallation Neutron Source), is to be installed at the MLF (Material Life Science Facility) in the J-PARC (Japan Proton Accelerator Research Complex) [1,2]. At the moment Hg target is bombarded by proton beams, rapid thermal heat deposition in mercury generates pressure waves, which propagate in the Hg and collide against the walls of the target vessel [3]. The target wall is excited by the pressure waves, and this causes negative pressure to develop along the wall. This negative pressure leads to cavitation erosion of the vessel wall [4–7]. In the JSNS, an intense proton-beam of 40 kJ per pulse with a pulse duration of approximately 1  $\mu$ s and a pulse rate of 25 Hz bombards the Hg target. Therefore, cavitation erosion, which degrades the cyclic fatigue strength of the vessel wall to a considerable extent, becomes a crucial factor that determines the structural integrity and a lifetime of the Hg target [8]. The MIMTM (Magnetic Impact Testing Machine) – a pulse generator driven by electromagnetic force – was developed to systematically examine the cavitation erosion, which is also known as pitting damage [9]. In an attempt to solve this problem by adopting a material approach, many kinds of conventional coatings were used and different surface improvements were made to

protect surfaces against the pit formation [10]. In general, hardened surfaces have good resistance against to pit formation [11].

On the other hand, the drastic change in the mechanical properties between the substrate and the improved surface layer was found to affect the interface strength between them, i.e., a large shear stress could be generated because of the mismatch between them. Among the various methods employed for surface improvements, plasma nitriding was found to be effective in preventing pitting damages for up to  $10^6$  cycles of impact [12]. However, when impact was applied for over  $10^6$  cycles, detached surface layers along the interface between the substrates and improved surface layers were observed. Recently, a novel method for surface improvement involving plasma nitriding and carburizing processes has been developed. In this method, the thickness and hardness distributions of the surface were optimized for mitigating the localized impact force [13,14].

In this study, a new coating method has been developed with the aim of preventing the formation of cracks on the substrate. The unique feature of this method is the formation of a double-layer coating that acts as a shock absorber on the substrate. FEM-analysis performed using the AUTODYN-2D code [15], which can solve the problems involving stresses between solids and fluids, shows the effectiveness of the SS/Au thin layer coatings in preventing the impact transmission to the substrate. The effectiveness of the SS–Au-double-layer-coated stainless steel plate in reducing the pitting damage was studied by fabricating a specimen using the diffusion bonding method and comparing the results of the

\* Corresponding author.

E-mail address: [masayoshi.kawai@kek.jp](mailto:masayoshi.kawai@kek.jp) (M. Kawai).

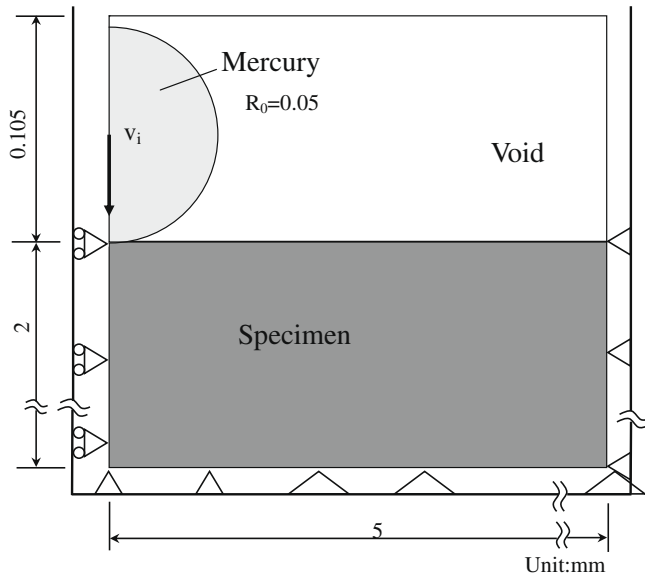


Fig. 1. Axisymmetric model for FEM-analysis of localized impact by micro-jet using the AUTODYN-2 code.

MIMTM impact test for the double-layer-coated SS plate and the no-coated SS plate.

## 2. Impact analysis

The pits on the wall of the target vessel are formed by the localized impact on the solid/liquid interface by the micro-jets and/or shock waves collision against the vessel wall. Micro-jet collision analysis was performed in the same manner as described in Refs. [16–18], by using AUTODYN-2D code to determine the magnitude of impact loading by micro-jet collision on the interface and the stress distribution in the multilayer composed of coating materials and the substrate. In other words, the ability of soft materials such as Au to absorb impact was investigated. An axisymmetric model, shown in Fig. 1, was adopted for calculation; this model comprised a micro-jet that was simulated using a spherical Hg-droplet and a flat solid plate. The model parameters were chosen so that the model yielded the same results as the MIMTM for experiments involving formation of the pitting hole by a 560 W impulse; the radius of Hg-droplet was 50  $\mu\text{m}$  and the micro-jet velocity,  $V_i$ , was

assumed to be 300 m/s. Three types of 2.0-mm-thick solid plates were considered: a 2.0-mm-thick single 316 type stainless steel (SS) plate, 0.1-mm SS/0.1-mm Au/1.8-mm SS and 0.05-mm SS/0.05-mm Au/1.9-mm SS. Material properties pertaining the Johnson–Cook model such as the static yield stress and work hardening coefficient were estimated by performing the inverse analysis on the load/depth curves measured by nanoindentation, a technique developed by the authors [19,20].

Fig. 2 shows the Mises stress distributions at 0.2 ms after the localized impact at  $V_i = 300$  m/s for (a) a single-layer of SS, (b) a 0.05-mm SS/0.05-mm Au SS plate, and (c) a 0.1-mm SS/0.1-mm Au SS plate. At 0.2 ms, the stress is maximized, and at this point, pit formation is observed in all three cases. It can be clearly seen that in case (a), the stress is transmitted into the substrate region, while in case (b), the stress develops along the surface layer, diminishes in the gold layer and reappears in the upper part of the substrate. In case (c), the stresses below the SS/Au interface is largely reduced, though weak stress is observed in the local region of the substrate. The stress exerted on the surface and the observed surface deformation are nearly the same in all cases.

Fig. 3 shows the change in the Mises stress at the representative positions as a function of the time elapsed after the impact. On the surface ( $d = 0.0$  mm), the stress is maximized after 0.02 ms; the maximum stress is calculated to be 1220 MPa for SUS, 1180 MPa for 0.1-mm Au, and 1100 MPa for 0.05-mm Au; these values are very close to one another, indicating that they would result in the formation of the pits with equal depths. It is noted that the thick Au layer experiences a large residual stress of approximately 1000 MPa after 0.45 ms at the ‘hot’ spot near the edge of red line beneath the deformed Hg drop shown in Fig. 2, since a major part of the stress has been exhausted to plastic deformation of the Au layer. At a depth of 0.05 mm, the interface between SS316 and the Au layers in case (b) experiences a large stress of approximately 600 MPa between 0.25 and 0.6 ms, however, such a high stress is not observed in cases (a) and (c). In particular, the stress observed in case (c) is 300 MPa until 2.5 ms and 50 MPa thereafter. At a depth of 0.2 mm depth, the peak stresses in cases (a) and (c) are almost identical ( $\sim 200$  MPa), while that the peak stress in case (c) is only 80 MPa.

These results show that the 0.1-mm-thick SS/Au coating absorbs stress to a sufficient extent and prevents fatigue in the SS substrate, while plastic deformation of the Au layer results in a large stress beneath the Hg drop. The results also indicate that the 0.05-mm-SS/Au coating does not mitigate the impact.

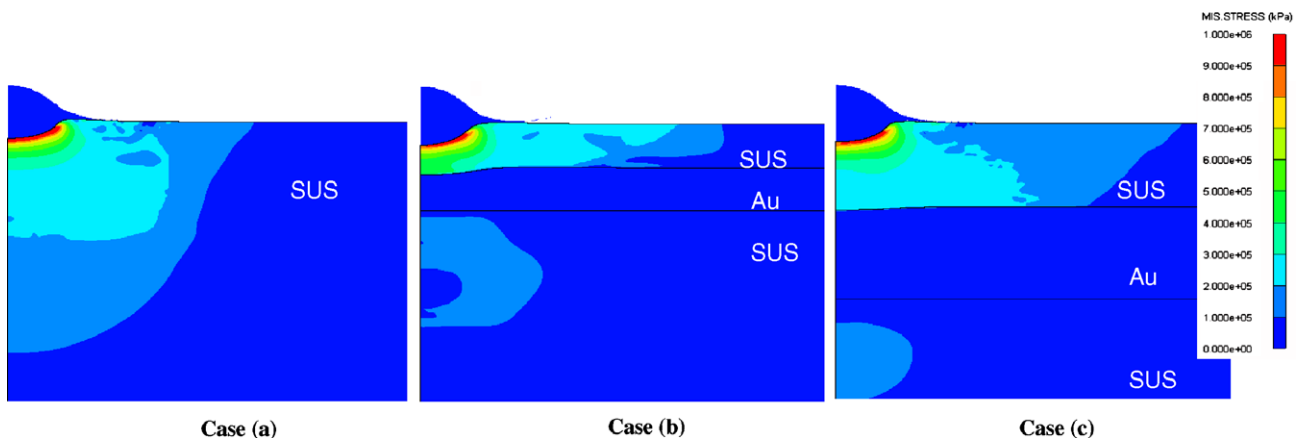


Fig. 2. Comparison of the Mises stress distributions at 0.02 ms after the localized impact at  $V_i = 300$  m/s. Case (a) SS only, (b) 0.5-mm SS/0.5-mm Au/SS and (c) 0.1-mm SS/0.1-mm Au/SS.

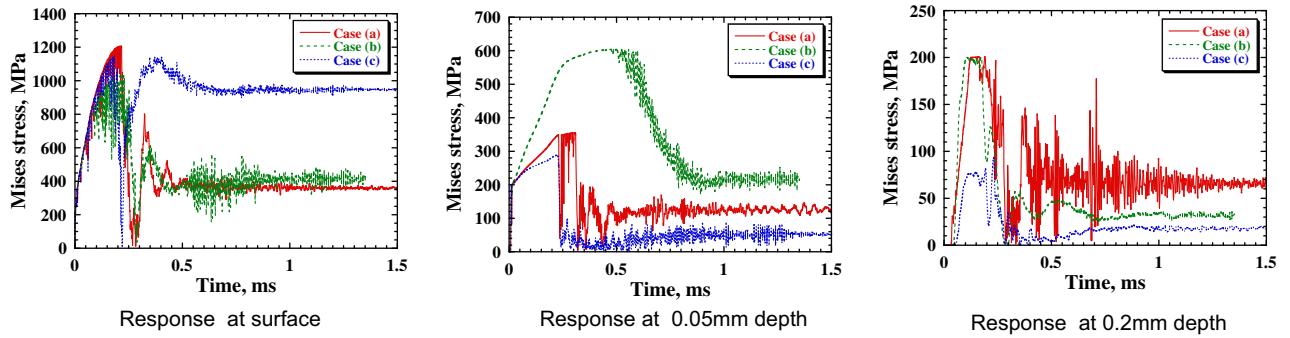


Fig. 3. Comparison of change in the Mises stress at the representative positions as a function of the time elapsed after the impact.

**3. Experiments**

The effectiveness of the SS/Au-double-layer coating in limiting the pitting damage was investigated by performing the impact experiments with the MIMTM with the no-coated and the double-layer-coated specimens.

*3.1. Fabrication of SS/Au/SS specimen*

Double-layer-coated specimens composed of 0.1-mm SS304, 0.1-mm Au and 3-mm SS304 with standard dimension of 60 mm × 60 mm were fabricated by the diffusion bonding method under the conditions of 900 °C × 4 h × 2.78 kgf/cm<sup>2</sup> in a small hot-press machine (FVHP-R). After diffusion bonding process, the specimens were confirmed to be defect-free by ultrasonic diagnostic

and EDS analysis. Fig. 4 shows the EDS mapping of regions including the Au layer on the left hand side and the substrate (SS304) layer on the right. The figure without material lacks indicates well bonding.

Fig. 5 shows the results of the EDS line analysis. The measured weight percent of Au in the Au layer is not 100% because of an error of 20% in measurements caused by noise. Consider two materials that are in contact at the interface  $x = 0$  at  $t = 0$ . The initial concentration  $C$  of a certain material is given by

$$C = C_0, x < 0, \quad C = 0, x > 0, \quad \text{for } t = 0. \tag{1}$$

According to a simple diffusion theory proposed by Crank [21], the concentration of the material at position  $x$  and time  $t$  from contact can be written as

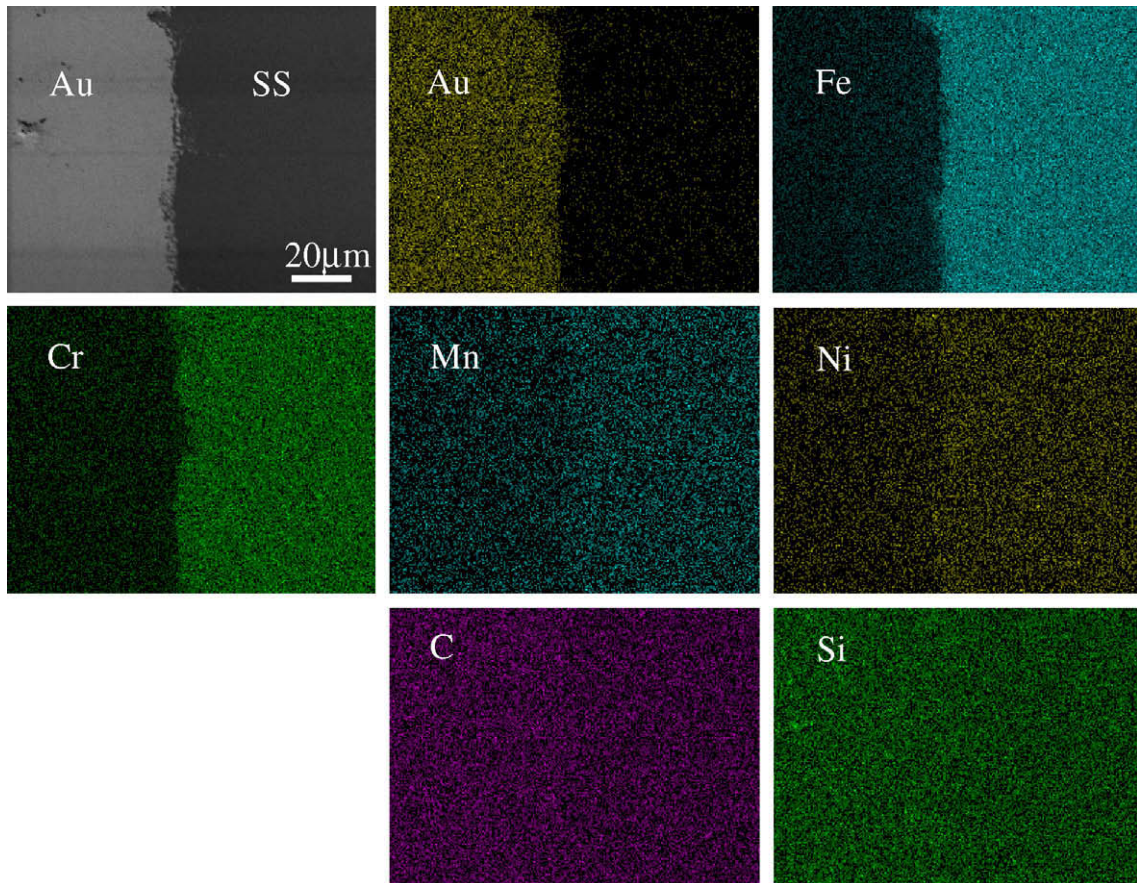


Fig. 4. Two-dimensional element distributions measured by EDS.



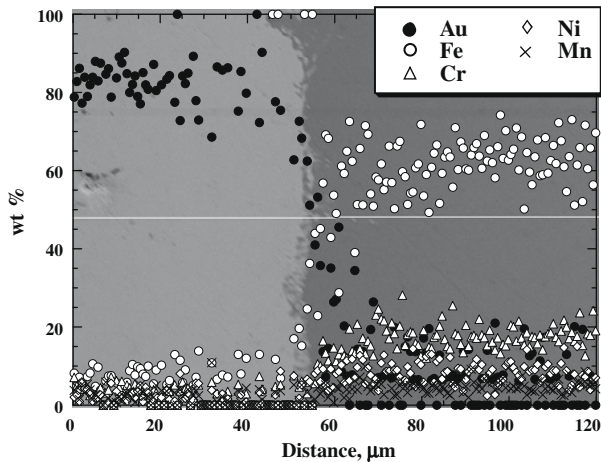


Fig. 5. One-dimensional element distributions measured by EDS.

$$c(x, t)/c_0 (x < 0, t = 0) = (1/2)\text{erfc}(x/2(Dt)^{1/2}). \quad (2)$$

From the figures, normalized Au diffusion line is read as 7.5  $\mu\text{m}$  layer thickness within the Au concentration range between 10% and 90%. From Eq. (2), the diffusion coefficient is estimated to be  $8.2 \times 10^{-17} \text{ m}^2/\text{s}$  according to the theorem stated in [21]. It can be said that this value is nearly equivalent to  $2.3 \times 10^{-16} \text{ m}^2/\text{s}$  estimated from the that of  $^{195}\text{Au}$  in  $\alpha \text{ Fe}$ :  $D(T) = 31 \times \exp(-62.4 \text{ (kcal/mol)/RT}) \text{ (cm}^2/\text{s)}$  [22], considering a difference between SS304 and  $\alpha \text{ Fe}$ . Fig. 6 shows the hardness distributions determined by using a dynamic ultramicrohardness tester (Shimadzu DUH-201S) with a Berkovich indenter with 3.0 gf and 0.15 gf/s. Hardness changes were observed over a wide region spanning nearly 100  $\mu\text{m}$ , which is far larger than the thickness of the diffusion layer determined from the EDS line analysis. It should be noted that increase in hardness is observed at positions deeper than 70  $\mu\text{m}$  in the substrate layer. These points are far from the Au/SUS304 interface; thus it is possible to avoid fracture due to brittleness near the interface.

### 3.2. Impact test with the MIMTM

Fig. 7 shows a Hg chamber and a specimen in the MIMTM. The inner diameter and height are 100 and 15 mm, respectively. The specimen is fixed at the center of the disk plate. Pulses of negative

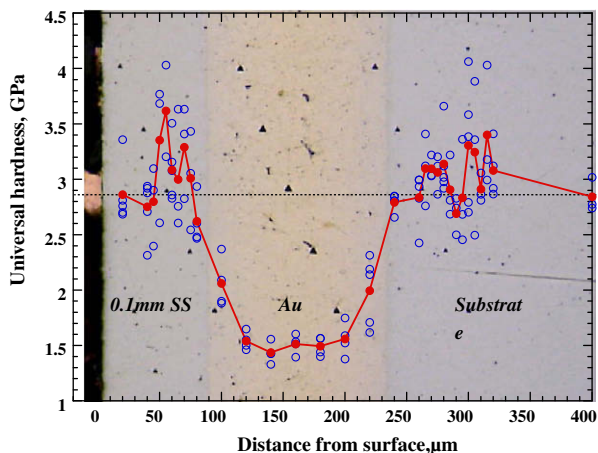


Fig. 6. Hardness distributions determined by using a dynamic ultramicrohardness tester (Shimadzu DUH-201S) with a Berkovich indenter with 3.0 gf and 0.15 gf/s.

pressure were applied on the Hg chamber through the disk plate driven with the striker, which is controlled in pressure strengths and repeat rates by the electromagnetic forces. The Hg cavitation was generated by the pulses of negative pressure very reproducibly. The magnitude of pressure was varied by varying the power supplied to the MIMTM. The morphology of pitting damage observed at a power of 560 W in the MIMTM was reasonably similar to that observed in proton-beam tests conducted using MW-class proton beams [9]. The repetition frequency of the pulses was 25 Hz, which was the same as that in the JSNS. The morphology and depth profile of the pits were observed by using a laser microscope and an SEM.

#### 3.2.1. Pitting damage

Fig. 8 shows cross-sectional micrographs of the damaged specimen of the SS/Au-double-layer-coated 304SS (SS/Au/SS) specimen after it was subjected to impacts for up to  $10^6$  cycles. The ruggedness of the surface increased with the number of impacts, and 25  $\mu\text{m}$ -deep pits formed by  $10^6$  impacts were observed on the surface. However, the interfaces between SS and Au were largely unaffected by these impacts, and no defect was observed in either Au layer or the substrate. A comparison of the results of laser microscopic observation of the SS316 single-layer plate and SS/Au-double-layer-coated SS plate is shown in Fig. 9. In the figures on the left, the surface features of the former appear more rugged than those of the latter. The pit-depth distributions on the right show that the deepest pits on the SS/Au/SS specimen and the single-layer SS specimen have the same depth (25  $\mu\text{m}$ ); however the majority of the pits on the SS/Au/SS specimen are shallower than those on the single-layer SS specimen.

In summary, it can be stated that 0.1-mm SS/0.1-mm Au-double-layer coating is more effective in reducing the number of pits formed on a surface and is expected to offer better protection from fatigue damage than does single-layer stainless steel.

## 4. Discussion

The experimental results showed that the 0.1-mm Au layer was an effective impact absorber and could be used to reduce fatigue in the substrate. Moreover, the pitting damage observed in the case of the substrate coated with a 0.1-mm-Au layer was lesser than that observed in the case of single-layer SS316. Since the mechanical properties of SS304 and SS316 were not very different from each other, test results could be considered to be reasonable for SS316.

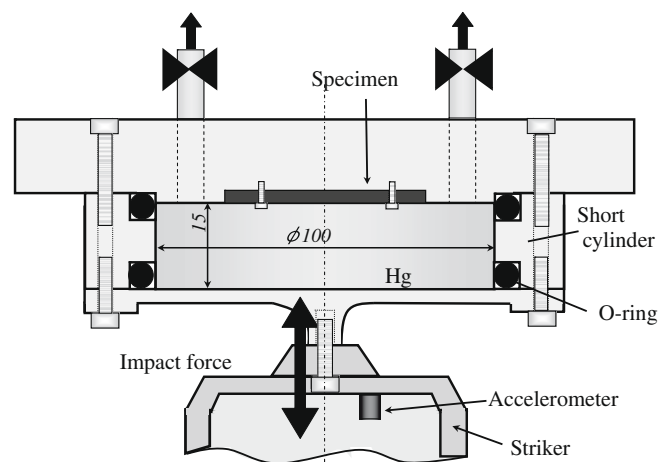


Fig. 7. Structure of the MIMTM impulse experimental apparatus.

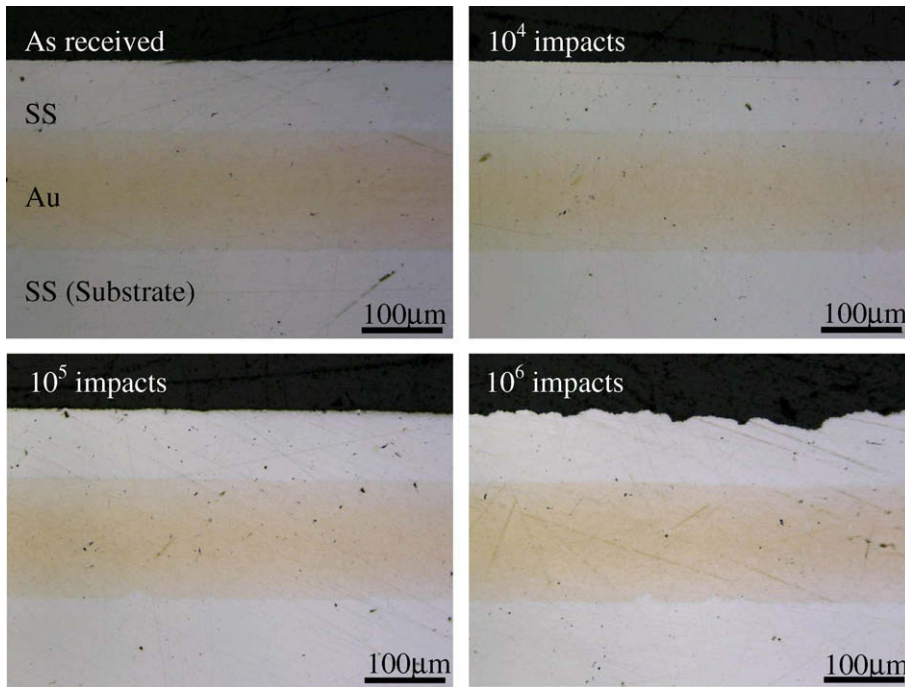


Fig. 8. Cross-sectional micrographs of damaged specimen of the SS/Au-double-layer-coated 304SS (SS/Au/SS) after impacts imposed up to  $10^6$  cycles.

However, these results are obtained for the case where impulses are applied for  $10^6$  cycles; the number of impulses applied in this case is two orders of magnitude lower than the number of impulses applied onto the actual JSNS target during a 2500 h of operation ( $2.25 \times 10^8$  cycles). Nevertheless, the specimen surface is damaged, and pits with depths of  $25 \mu\text{m}$  are present on the surface; this depth is at most 1/4th of the thickness of the SS layer.

Therefore, it is required that the top layer of SS be substituted with materials harder than SS or be subjected to surface treatment in order to strengthen the material.

The other problem that will be encountered when Au is used as a shock absorber is radiation hardening of Au, as pointed out by Hamaguchi et al. [23]: Au alloy (75Au–9Ag–16Cu) samples tested at  $150^\circ\text{C}$  (Y06) and  $200^\circ\text{C}$  (Y02) after proton irradiation in the

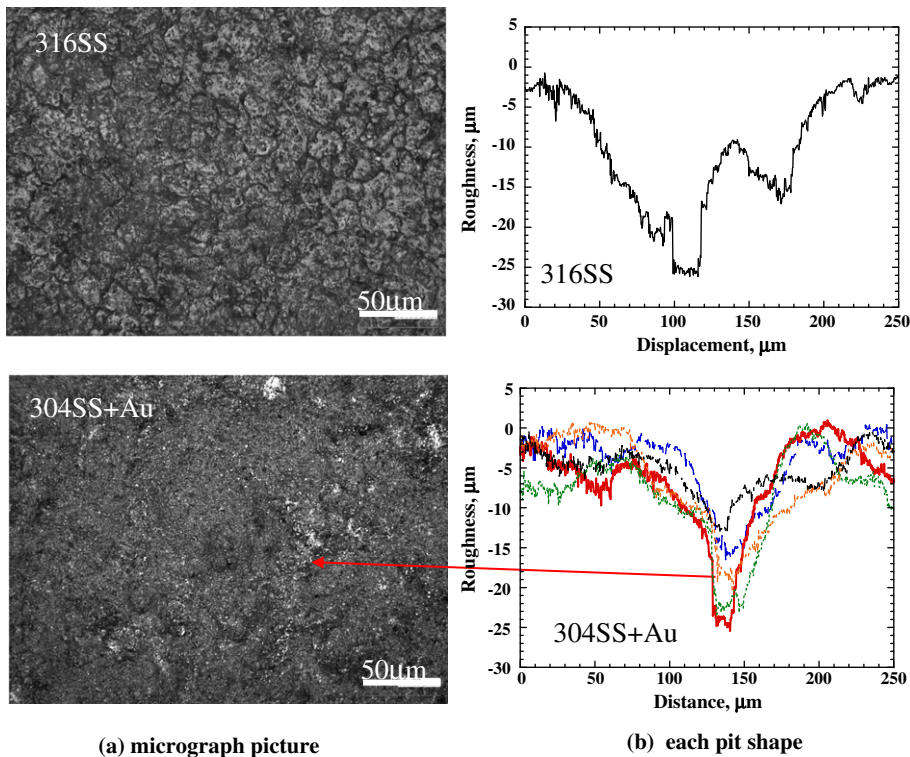


Fig. 9. Comparison of laser microscopic observation of the specimens after impacts imposed up to  $10^6$  cycles.

STIP-II experiments [23] showed significant loss of strength, similar to embrittlement, although the Pt samples showed good tensile strength and tensile elongation before the irradiation. Therefore, other materials should be used as shock absorbers. Materials that can be possibly be used are soft metals such as Cu, Al, Zn, Sn and Pb, or highly damping materials. These damping materials include those with a magnetic component in their structures (Fe, Ni alloys based on Fe and on Co and Ni) and those with reversible martensite in their structures, such as alloys based on the following systems: Ni–Ti, Cu–Mn, Cu–Al, Cu–Zn, Cu–Sn, Au–Cd, Fe–Pt, ( $\sim$ +B)-alloys of the martensitic class based on Ti, etc. [24].

To summarize, the role of the shock absorber in reducing the pitting damage, particularly to the substrate, is investigated in the present analysis and experiments are performed using impulses of  $10^6$  cycles. It is interesting to study the different types of damage that can be caused by impulses of more than  $10^6$  cycles: surface coat damage, chemical reactions between the material of the second layer and Hg, and cracks on the substrate. This topic must be studied in greater detail in the future to confirm that double-layer-coated SS can be used to construct target vessels. Additionally, methods fabricating three-dimensional targets are also expected to be of considerable importance in the future.

## 5. Conclusion

Liquid-Hg target systems for MW-class spallation neutron sources suffer pitting damage caused by cavitation, which is induced by the pressure waves generated by the injection of high-intensity proton beams. Localized impacts caused by micro-jets, which are generated by cavitation-bubble collapse, result in pitting damage to the target vessel wall. A 0.1-mm SS/0.1-mm Au/3-mm SS plate was fabricated by the diffusion method. Using the double-layer-coated SS plate, the stress on the substrate could be reduced by a considerable extent. Under the 560 W impulse applied for within the  $10^6$  cycles by the MIMTM, pits produced on the surface of the double-layer-coated plate were shallower than those produced on the single-layer SS plate.

Thus, it can be concluded that pitting damage caused to wall of the target vessel can be effectively reduced by coating two layers; composed of top layer of hard metal and the second of a soft metal, on the substrate. However, pitting damage should be reduced even when impulses are applied for more than  $10^6$  cycles. Further investigation on the use of materials other than Au (e.g. Cu or Ni) as shock absorbers will be carried out for the case where impulses are applied for  $10^8$  cycles. A suitable method of fabrication of a three-dimensional target vessel will also be proposed.

## Acknowledgement

This research was partly supported by a Grant-in-Aid in Scientific Research by the Japan Society for Promotion of Science, Nos. 19106017 and 17360085.

## References

- [1] S. Nagamiya, Neutron News 16 (1) (2005) 16–19.
- [2] Y. Ikeda, Neutron News 16 (1) (2005) 20–24.
- [3] M. Futakawa, K. Kikuchi, H. Conrad, H. Stechemesser, Nucl. Inst. Meth. Phys. Res. A439 (2000) 1–7.
- [4] M. Futakawa, H. Kogawa, R. Hino, J. Phys. IV France 10 (2000), Pr9-237–242.
- [5] M. Futakawa, H. Kogawa, R. Hino, H. Date, H. Takeishi, Int. J. Imp. Eng. 28 (2003) 123–135.
- [6] J.R. Haines, K. Farrell, J.D. Hunn, D.C. Lousteau, L.K. Mansur, T.J. McManamy, S.J. Pawel, B.W. Riemer, Summary of Mercury Target Pitting Issue, SNS-101060100-TR0004, 2002.
- [7] M. Futakawa, T. Naoe, C.C. Tsai, H. Kogawa, S. Ishikura, Y. Ikeda, H. Soyama, H. Date, J. Nucl. Mater. 343 (2005) 70–80.
- [8] M. Futakawa, T. Wakui, H. Kogawa, Y. Ikeda, Nucl. Inst. Meth. Phys. Res. A562 (2006) 676–679.
- [9] M. Futakawa, T. Naoe, H. Kogawa, C. Tsai, Y. Ikeda, J. Nucl. Sci. Technol. 40 (2003) 895–904.
- [10] M. Futakawa, T. Naoe, H. Kogawa, S. Ishikura, H. Date, J. Soc. Mater. Sci. 53 (2004) 283–288 (in Japanese).
- [11] R. Garcia, F.G. Hammitt, R.E. Nystron, Am. Soc. Test. Mater. (1967) 239–283.
- [12] T. Naoe, T. Oi, H. Kogawa, T. Wakui, M. Futakawa, J. Soc. Mater. Sci. Jpn. 57 (2) (2008) 159–166 (in Japanese).
- [13] T. Naoe, M. Futakawa, T. Shoubu, T. Wakui, H. Kogawa, H. Takeuchi, M. Kawai, J. Nucl. Sci. Technol. 45 (2008) 698–703.
- [14] M. Kawai, H. Kokawa, M. Michiuchi, H. Kurisihita, T. Goto, M. Futakawa, T. Yoshiie, A. Hasegawa, S. Watanabe, T. Yamamura, N. Hara, A. Kawasaki, K. Kikuchi, J. Nucl. Mater. 377 (2008) 21–27.
- [15] AUTODYN Theory Manual, Ver. 4.1, Century Dynamics, Inc., 2000.
- [16] S. Ishikura, H. Kogawa, M. Futakawa, M. Kaminaga, R. Hino, M. Saito, Trans. Atom. Energy Soc. Jpn. 3 (1) (2004) 59–66 (in Japanese).
- [17] T. Naoe, M. Futakawa, T. Oi, S. Ishikura, Y. Ikeda, J. Soc. Mater. Sci. 54 (11) (2005) 1184–1190 (in Japanese).
- [18] M. Futakawa, T. Naoe, H. Kogawa, H. Date, Y. Ikeda, JSME Int. J. A 48 (4) (2005) 234–239.
- [19] M. Futakawa, T. Wakui, Y. Tanabe, Stress–strain relationship evaluation by load–depth curve obtained from indentation technique, in: Proceedings of the 10th APNDT, September 17–21, 2001, Brisbane, Australia, 2001 (CD-ROM).
- [20] M. Futakawa, T. Wakui, T. Naoe, I. Ioka, J. JSEM 4 (3) (2004) 222–227 (in Japanese).
- [21] J. Crank, Mathematics of Diffusion, Oxford University Press, 1975.
- [22] The Japan Institute of Metals Compile, Metal Databook, third ed., 1974, p. 25 (in Japanese).
- [23] D. Hamaguchi, Y. Dai, K. Kikuchi, S. Saito, S. Endo, M. Kawai, Mechanical Property Changes on Au and Pt Alloys Irradiated by High Energy Proton, Presented in the Present Workshop.
- [24] S. Yu. Kondrat'ev, G. Ya Yaroslavskii, B.S. Chaikovskii, Classification of High-damping Metallic Materials, Leningrad Polytechnic Institute, Institute of Strength Problems, Academy of Sciences of the Ukrainian SSR, Kiev, Translated from Problemy Prochnosti, No. 10, 32–36, October, 1986, <<http://www.springerlink.com/content/h1811t08658064ll/fulltext.pdf>>.